

Biographies

Juan Ceva obtained a B.S. degree in Aerospace Engineering at St. Louis University and a M.S. and Engr. degree in Aeronautics and Astronautics at Stanford University. As a graduate student of Professor Parkinson and as a summer intern at the Jet Propulsion Laboratory (JPL), he has worked on a variety of topics involving GPS, in particular WAAS (the topic of his Engineer thesis).

Willy Bertiger received his Ph.D. in Mathematics from the University of California, Berkeley, in 1976. In 1985, he began work at JPL as a Member of the Technical Staff in the Earth Orbiter Systems Group. His work at JPL has been focused on the use of GPS for high precision orbit determination and positioning.

Ronald Muellerschoen received a B.S. degree in physics at Rensselaer Polytechnic Institute and a M.S. degree in Applied Mathematics at the University of Southern California. He is currently a Member of the Technical Staff in the Earth Orbiter Systems Group at the Jet Propulsion Laboratory (JPL). His work at JPL has concentrated on the development of efficient filtering/smoothing software for processing GPS data and the processing of Topex/Poseidon-GPS data.

Tom Yunck received his B.S.E.E. from Princeton University, and his Ph.D. in Systems and Information Science from Yale University. He is currently Deputy Manager of the Tracking Systems and Applications Section at JPL, where he is involved in the application of GPS to precise orbit determination and geodesy.

Bradford Parkinson is Professor at Stanford University and is Program Manager of the Relativity Gyro Gravity Probe B Experiment, which utilizes GPS extensively. He served as the first Program Director of the GPS joint Program Office, and was instrumental in the system's development. He is a past chairman of the ION Satellite Division, and 1991 winner of the Kepler Award.

Abstract

A powerful dynamical technique to compute precise GPS satellite orbits for the FAA real-time Wide-Area Augmentation System (WAAS) has been evaluated. The dynamical technique estimates GPS satellite states from a long history of measurements, which are related estimate through precise models of satel-

lite dynamics. This contrasts with nondynamical techniques, in which an inverted form of the navigation fix solution yields the instantaneous position of the satellite, without introducing dynamical information. The dynamical orbit determination method not only yields much more accurate and robust orbit solutions, it enables complete separation of orbit and satellite clock errors. Results with real data show that a network of 12 monitor stations distributed over the continental U.S. and Canada, producing dual frequency pseudorange data, yields orbit accuracies of better than one meter within the service volume, as compared with the JPL precise ephemerides. This is about a factor of 6 improvement over the broadcast ephemerides.

In a WAAS simulation the dynamical orbit estimation technique produced the most accurate user results. Over the 30 simulated users, the mean of the eastern, northern and vertical components of the users' standard deviations were 5.13 cm east; 5.36 cm north; and 9.15 cm vertical. This represents the orbit and clock components of the user position error. No latency, tropospheric, or User measurement errors are included in the simulated user ranges (although measurement errors were of course present in the data used to compute the orbits). A comparison with the results obtained with the broadcast and non-dynamical orbits is presented.

The dynamical orbit estimation process, the slow correction generation, and its broadcast can be done in 2.5 seconds. Real-time performance of the dynamical orbit estimation is easily achievable in a WAAS scenario.

1 Introduction

The Federal Aviation Administration (FAA) is currently developing a GPS-based navigation system that is intended to become the primary navigation aid for commercial aviation during all phases of flight - including Category I precision approach. This revolutionary navigation system will be based on the concept of WAASGPS (Kee 1993). Called by the FAA the Wide-Area Augmentation System (WAAS), it will make use of a network of 20 to 30 Wide-area Reference Stations (WRSs) distributed throughout the National Airspace System. These reference stations will collect pseudorange and atmospheric measurements, and will send them to one, or perhaps more, Wide-area Master Stations (WMSs). The WMS will process the data to

provide a *vector correction* for each GPS satellite. The vector correction will include as separate components the GPS ephemeris errors, satellite clock bias and ionospheric delay estimate. The FAA distinguishes two kinds of corrections: a *slow correction* and a *fast correction*. The slow correction contains, as its name indicates, the slowly varying errors—the ephemeris error. Due to its slowly varying nature, this error need be transmitted only every 5 minutes. On the other hand, the satellite clock error is quickly varying in nature due to SA—and demands a faster correction rate, on the order of one correction message every six seconds. The corrections will be sent to the users by means of a Geosynchronous Earth Orbit (GEO) satellite using a signal and data format designed by RTCA¹ Special Committee 159. The WAAS is expected to provide supplemental radionavigation by the year 1997, and eventually to become the primary system of navigation. The system will add to the current GPS system the following features: a ranging function that will improve *availability* and *reliability*; differential GPS corrections that will improve *accuracy*; and *integrity* monitoring that will enhance safety. To meet the requirements associated with a primary navigation system, WAAS should be able to provide fault-free position fix with a *minimum availability* of 0.999 for Category 1 approach, and 0.99999 for domestic *en route*, terminal and non-precision approach phases of flight.

Section 2 describes dynamical orbit determination and assesses the accuracy of the GPS ephemeris obtained using this technique. Section 2.3 presents the user positioning accuracy obtained in a WAAS scenario simulation. Section 3 discusses the advantages that a dynamical orbit determination introduces over non-dynamical techniques. The real-time aspects of a dynamical orbit determination technique are mentioned in Section 4. The conclusions are drawn in Section 5.1.

2 Dynamical Orbit Determination

By dynamical orbit determination we refer to a technique that computes precise satellite orbits from a collection of measurements that are related to the satellite states by precise dynamical models that carefully described the orbital motion of the satellite. The relationship between satellite states and observables are non-linear in nature. The commonly implemented sta-

tistical estimation technique requires linear relationships between states and observables; therefore, the equations describing the motion of the satellite are linearized with respect to a nominal trajectory.

2.1 State vector, numerical propagation models and orbit estimator

Our solutions for the GPS ephemeris are implemented in a software set referred to as Gipsy/Oasis II (GOA 11). The filter implementation is a Square Root Information Filter (SRIF) which yields increased numerical stability compared to non-square root implementations (Cf. Bierman (1977), Wu et al. (1990)). If there are 110 numerical problems it is equivalent to other Kalman implementations.

When solving for GPS ephemeris errors, our state vector consists of a GPS epoch state, GPS clock, station troposphere, and station clocks. One station clock is held as reference. Station tropospheres are treated as random walks. We use 30 hours data arcs in the solutions represented in this paper. The epoch state for GPS refers to the position and velocity at the beginning of the 30 hour arc for GPS.

For the dynamical ephemeris solution no process noise is added to the GPS epoch state (position and velocity). In a real time implementation, the filter would be slightly modified to work on a current state rather than an epoch state and a small amount of process noise would be added to the current state to account for imperfect dynamics when the arc length was long compared to the accuracy of the dynamic model. For the tests here, no process noise on the state is necessary due to the short 30 hour data arcs.

For the non-dynamical ephemeris adjustments, an acceleration vector is added to the filter state for each GPS with a white noise update at each measurement time. The amount of noise at each measurement time is so large that the position solutions for GPS are uncorrelated.

As the dynamical model improves, less process noise is necessary on the GPS current states in a real time implementation. Smaller process noise means that you get to average out other error sources using dynamics. Here we use the current state of the art GPS dynamical models which include:

- A 12 x 12 expansion of the JGM-3 gravity model (Watkins et al. 1994).

¹Radio Technical Commission for Aeronautics.

- Third-body effect for the Sun and the Moon only (Newhall, Standish & Williams 1983).
- No relativistic gravitational perturbation.
- Solid Earth tide (Wahr 1981) and ocean tide (Nerem 1994) models.
- Direct solar radiation pressure model (Fliegel & Gallini 1992).
- No Earth albedo perturbation.
- No Atmospheric drag perturbation.

2.2 WAAS dynamical orbit determination results

A network of tracking stations was selected across the continental U. S. and Canada (with the exception of Bermuda) (see Fig. 1 and Table 1). These tracking stations, that represent the Wide-Area Remote Stations or WRSs in a WAAS network, belong to the JPL global network of GPS receivers and are equipped with JPL Turbo-Rogue receivers. From these stations "real" carrier-smoothed pseudorange measurements² were collected thirty seconds apart during a period of thirty hours on January 10, 1995. The estimation method selected was the one that implements numerical propagation of the dynamical models together with a position-velocity state vector as described in Sec. 2.1. The tropospheric delay error was not estimated; in its place, the estimated values obtained from the JPL precise ephemerides were used³. The initial spacecraft state was taken from the results of the precise orbits⁴.

²The JPL Turbo-Rogue receivers already output carrier-smoothed pseudorange, saving one step in the data processing.

³This was done in anticipation of the user positioning simulation presented in Sec. 2.3. In this simulation, the measurements are generated using the precise JPL ephemeris. The use of the same tropospheric estimates in both the orbit estimation process and the user positioning simulation assures a perfect cancellation of the tropospheric delay bias that although of great importance, is not the main interest of this research.

⁴Of course this cannot be done in the real-time application, however in the worst case, one could always start the orbit estimation process with an initial state based on the broadcast ephemerides that are always available. Also, the use of accurate dynamical models permits the propagation of the orbits when new measurements are not available; in the case of the JPL precise ephemerides, the orbital errors remain under one meter even when propagated three days ahead without incorporating new observations.

2.2.1 Comparison with the JPL precise orbit

An indication of the accuracy of the estimated orbit is to compare the results with another estimated orbit known to be more precise. In this case the results of the GPS orbits for January 10, 1995, obtained with the WAAS network were compared with the JPL precise GPS orbits with a $3\text{-D } 1\sigma$ accuracy of 20 cm (Zumberge et al. 1995). Table 2 shows the RMS differences between the orbits over the service area of the WAAS network in the radial, long-track, and out-of-plane orbital components. Carrier phase measurements would

The WAAS Dynamical Orbit Accuracy	
Orbit component	Accuracy (m, 1σ)
Radial	0.65
Cross-track	0.75
Long-track	1.6

Table 2: The WAAS dynamical orbit accuracy. The accuracy is established as the difference between the orbit estimated using the WAAS stations and dynamical information and the JPL precise orbit over the service area of the WAAS network.

undoubtedly improve the solution (Yunck et al. 1995), but they should not be used according to the WAAS specifications (FAA 1994). Post-process smoothing of the resulting orbit is not suitable for a real-time application. OK

2.2.2 Comparison with the broadcast orbit

The dynamical orbit generated with the WAAS network shows a fourfold improvement over the broadcast orbit. The broadcast orbit for December 10, 1995, was differenced with respect to the JPL precise orbit in the same manner as before. Table 3 shows the RMS differences between the orbits over the service area of the WAAS network in the radial, along-track, and out-of-plane orbital components.

Given the high quality of the broadcast orbit, we believe that there are no SA effects imposed on them (Zumberge & Bertiger 1996). However, if SA were to degrade the broadcast orbits, the need of an independent ephemeris source such as the one presented here would be imperative to maintain the accuracy required by WAAS.

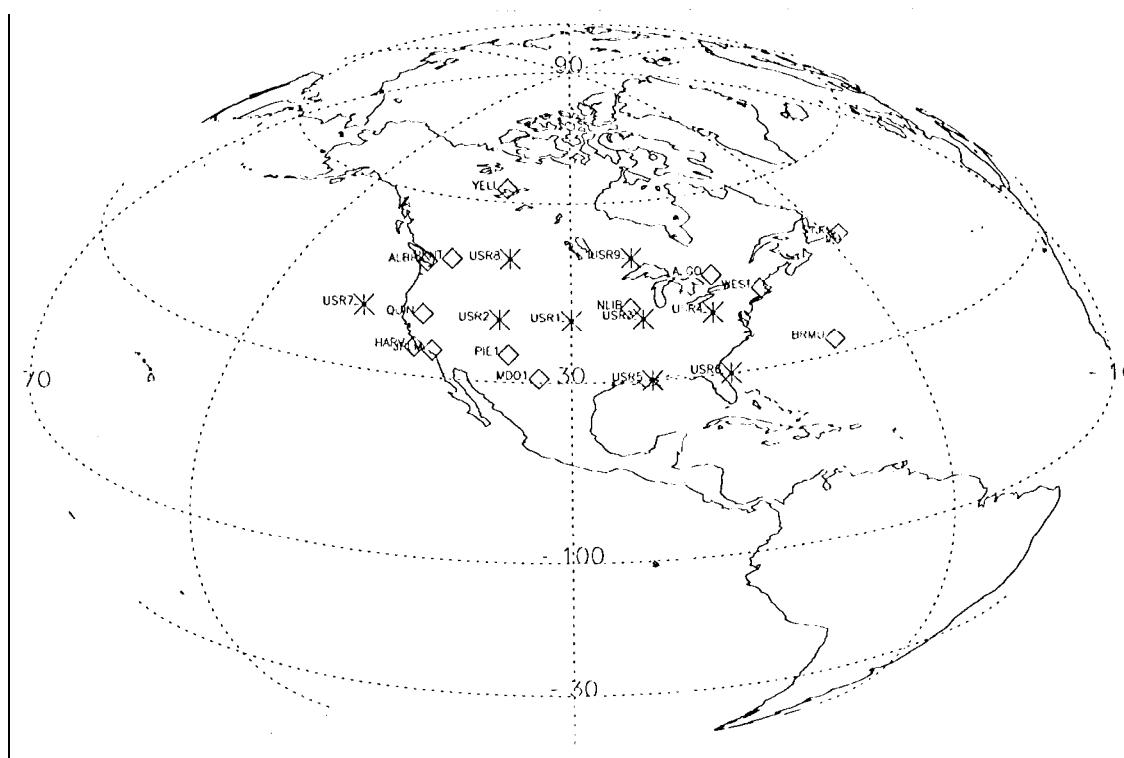


Figure 1: The WAAS simulated network. The WRSs are symbolized with diamonds. Users were placed in the locations represented by asterisks as well as in the vicinity of the WRSs with the exception of Bermuda.

The Broadcast Orbit Accuracy	
Orbit component	Accuracy (m, 1σ)
Radial	1.7
Cross-track	2.6
Long-track	7.4

Table 3: The broadcast orbit accuracy. The accuracy is established as the difference between the broadcast orbit and the JPL precise orbit over the service area of the WAAS network.

2.3 The WAAS user positioning simulation

A simulation was conducted to assess the improvement that the dynamical orbit estimation technique offers to the WAAS users. In it, nine static users were distributed (see Table 1) within the simulated WAAS

network depicted in Fig. 1, and additionally, another eleven users were placed over twelve of the thirteen (all but Bermuda) WRSs on the network.

The range observables were created by computing geometric ranges from the users to the GPS satellite positions as prescribed by the JPL precise ephemeris for the period of January 9, 1995, 23:59:50 GMT to January 10, 1995, 23:58:50 GMT. The purpose of the simulation was to assess only the contribution of the orbit accuracy to the user positioning error after performing the slow and fast corrections. No noise was added to the generated measurements; no ionospheric delays were included, and furthermore, the tropospheric delay biases were removed by using the JPL precise orbit tropospheric biases for that day. These atmospheric biases (especially the ionospheric) together with S/A and latency⁵, are the dominant error sources, but are

⁵ A previous study of the latency effect is reported in Yunck et al. (1995). In this study the effect of the user extrapolation of his/her last fast correction under the effect of SA is addressed.

The WAAS Simulated Network Station and User Locations					
Type	4 char. ID	City	Country	Latitude (deg)	Longitude (deg)
WMS & USR	ALBH	Albert Head	Canada	48.39	-123.49
WMS & USR	ALGO	Algonquin	Canada	45.96	-78.07
WMS	BRMU	Bermuda	U. K.	32.37	-64.70
WMS & USR	HARV	Halvest Platform	USA	34.47	-120.68
WMS & USR	JPLM	Pasadena	USA	34.20	-118.17
WMS & USR	MDO1	McDonald	USA	30.68	-104.0]
WMS & USR	NLIB	North Liberty	USA	41.77	-91.57
WMS & USR	PENT	Penticton	Canada	49.32	-119.62
WMS & USR	PIT1	Pic Town	USA	34.30	-108.12
WMS & USR	QUIN	Quincy	USA	39.97	-120.94
WMS & USR	STJO	Saint John's	Canada	47.60	-52.68
WMS & USR	WEST	Westford	USA	42.61	-71.49
WMS & USR	YELL	Yellowknife	Canada	62.48	-114.48
USR	USR1		USA	40.00	-100.00
USR	USR2		USA	40.00	-110.00
USR	USR3		USA	40.00	-90.00
USR	USR4		USA	40.00	-80.00
USR	USR5		USA	30.00	-90.00
USR	USR6		USA	30.00	-80.00
USR	USR7		USA	40.00	-130.00
USR	USR8		G n a d i	50.00	-110.00
USR	USR9		Canada	50.00	-90.00

Table 1: The WAAS simulated network station and user locations.

not the topic of interest in this study.

To simulate the slow and fast corrections, the following steps were taken:

1. Using the previously estimated dynamical orbit from the WAAS network, the satellite position component of the simulated pseudorange was subtracted. This is the so-called slow correction. Note that since the orbit generated by the WAAS network and the JPL precise orbit differ, some ephemeris error remains. It is precisely how this ephemeris error translates into user positioning error that is of interest in this simulation. (Recall that the orbit correction is performed with real data.)
2. The tropospheric delay values that the JPL pro-

The study concludes that (after using different extrapolation techniques, involving the use of pseudorange and combinations of pseudorange and phase as well as linear and quadratic models) a linear extrapolation with pseudorange data alone will not suffice and suggest the introduction of phase data that improves the scatter by an order of magnitude.

cise orbit provided for that day were subtracted from the measurements. Since these are the same values that went into the WAAS orbit estimation, a perfect cancellation took place. This helps to isolate the ephemeris and clock errors.

3. The clock biases were estimated from the measurements once the slow corrections (and the tropospheric delay biases) were removed. This is the so-called fast correction, for the satellite clock biases are dominated by SA that is fast changing in nature.
4. An estimator was run to estimate the user location. The coordinates of the location were estimated as white noise stochastic parameters, essentially solving for a point positioning at every epoch as it would be more characteristic of a moving user, e.g., an airplane. The standard deviation of the point positioning history was computed for every station along eastern, northern and vertical components. The mean of the standard deviation of all stations was also computed in the eastern,

northern and vertical components. The typical VDOP value was in the order of 1.2

The vertical component is the one of interest, for it is the hardest to determine and the most stringent requirement in the IVA landing category specifications. Figure 2 and Table 4 show the standard deviation of the RMSs of all stations when using the WAAS network dynamical orbit, and, for comparison, the results when using the broadcast orbit. It can be seen in the figure, that the WAAS dynamical orbit results in a mean standard deviation of the vertical error of 9.15 cm (1σ). It must be emphasized that these results do not include the dominant source of error for single frequency users, namely, the ionospheric delay. However, using ionospheric delay estimation algorithms such as the one presented in Mannucci, Wilson & Edwards (1993) the ionospheric delay can be estimated within an accuracy of half a meter (Mannucci, Wilson & Yuan 1994). In any event, the WAAS dynamical orbit considerably improves the user positioning when compared with the broadcast orbit that has a vertical error of 38.6 cm (1σ). As Table 5 shows, the introduction of dynamical information prevents the degradation of the user positioning on the periphery of the network.

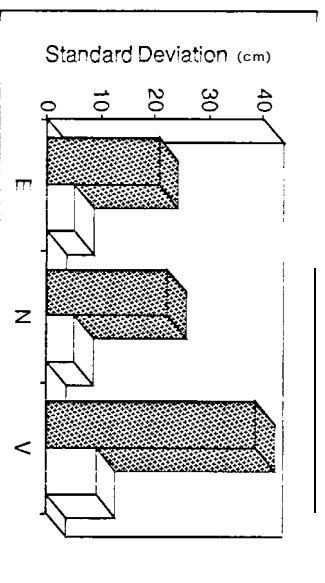


Figure 2: Results of the WAAS user positioning simulation. The numbers show the mean standard deviation in the eastern, northern and vertical components of the point positioning history of the simulated WAAS users. The results obtained with the WAAS network generated dynamical orbit (white bars) are contrasted with the results achieved using the broadcast orbit (dark bars).

2.4 Conclusion

The dynamical orbit generated with the simulated WAAS network results in user positioning accuracies that not only exceed the requirements of the IVA category I approach, but that are also closer in accuracy to the more demanding category II approach. The introduction of dynamical information prevents the degradation of the user solution in the periphery of the network as is the case with nondynamical techniques. Finally, the ability of the proper separations between clocks and ephemeris errors permits the usage of the slow/fast scheme that is demanded in the IVA WAAS specifications.

3 Improvement Over Nondynamical Techniques

The dynamical orbit determination contrasts with the nondynamical technique, in which an inverted form of the navigation fix solution yields the instantaneous position of the satellite, without introducing dynamical information. It also contrasts with a kinematic technique (Tsai et al. 1995) in which the first time-derivative of the satellite position error is also estimated, again without the use of dynamics.

Some fundamentals of satellite range tracking must be understood to appreciate the superiority of the dynamical techniques. Orbit estimation sensitivity with differential techniques as well as clock and ephemeris range bias separation are among these fundamental aspects.

3.1 Nondifferential and differential satellite tracking

Figure 3 shows that when a single station tracks a satellite, the tracking station is less sensitive to along-track and cross-track motion and mostly senses radial motion. In the example illustrated in Fig. 4, two stations difference their range measurements to a commonly viewed satellite. In this case the sensitivity reverses; now the differenced measurements are not sensitive to radial displacements (along the bisecting line of the angle subtended by the satellite and the stations) but only to motion parallel to the baseline. This is proven mathematically (for the 2-1 case) in Section 3.2.

It is also important to note that when several stations

The WAAS User Positioning Summary Results			
Orbit Type	East (cm, 1 σ)	North (cm, 1 σ)	Vertical (cm, 1 σ)
WAAS Dynamical	5.13	5.36	9.15
Broadcast	20.7	22.2	38.6

Table 4: Results of the WAAS user positioning simulation. The numbers show the standard deviation in the east, north and vertical components of the RMSs of the point positioning history of the simulated WAAS users. The dynamical orbit results are contrasted with the ones obtained using the broadcast orbit

observing a commonly viewed satellite try to solve for the unknowns or the system, namely, the position of the satellite, its clock bias, and the station clock biases, two options exist: the first one calls for the elimination of the satellite clock by differencing the measurements; the second calls for omitting one of the station clocks from the list of unknowns, *de facto* referencing all the station clocks to the one omitted. The first of the approaches has performed an obvious differentiation of the measurements, and the second one has performed an identical differentiation in a more subtle way by referencing all the clocks to a reference one omitted from the solution⁷. In both cases the network of stations is virtually insensitive to satellite radial displacements, being able to observe properly transverse motion only.

3.2 The 11D1 {1} concept

The User Differential Range Error (UDRE) is defined (FAA 1994) as "the 99.9% accuracy of the corrections for the designated satellite, indicating the accuracy of combined fast and slow corrections, not includ-

⁶ Both of these approaches are mathematically equivalent (Wells, Doucet & Lindlohr 1986, Grafarend & Schaffrin 1986). Kuang, Schutz & Watkins (1995) show that estimating the receiver clock error and eliminating the bias by differencing the measurements at each measurement epoch are mathematically equivalent, provided that no *a priori* clock information is used in the undifferenced case.

⁷ Consider the example in which two tracking stations of known positions obtain range measurements to a commonly visible satellite. The system contains five unknowns, namely, the three components of the satellite position, its clock bias and the two station clock biases. In the second case, the two measurements from stations to satellite are not differenced, one reference station is selected and its clock bias is eliminated from the list of unknowns. This leaves two measurements and five unknowns or a $5 - 2 = 3$ deficiency. In the first case mentioned, the two measurements are differenced, reducing the number of measurements to one, eliminating the satellite clock and leaving the difference between station clocks as an unknown together with the satellite position. Again, an identical $4 - 1 = 3$ deficiency exists

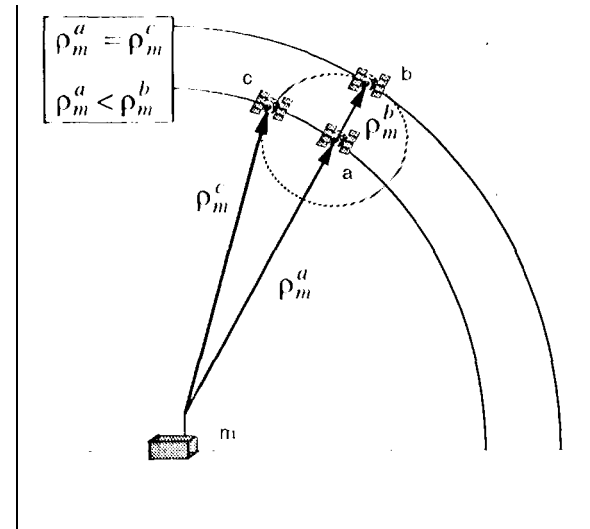


Figure 3: Nondifferential GPS tracking sensitivity. A single satellite is being tracked by a monitor station m . The station cannot distinguish between positions a and b (lateral motion), and can only sense vertical motion such as changes from position a to position b .

ing the accuracy of the ionospheric corrections. The ephemeris accuracy component is an 'equivalent' range accuracy for the worst location in the coverage region." The combined error due to slow and fast corrections will be smaller than the absolute range error from just the slow ephemeris error (Yunck et al. 1995). The ephemeris component of the UDRE can be calculated by computing the sensitivity of the range measurement to the satellite position. According to Fig. 5, it can be shown (Yunck et al. 1995) that the sensitivities of the range r_u^k with respect to satellite height H and lateral position L are given by

$$\frac{\partial r_u^k}{\partial H} = \frac{h}{r_u^k} = \cos \theta, \quad (1)$$

The WAAS User Simulation Results			
[4 char. ID	East (cm, 1 σ)	North (cm, 1 σ)	Vertical (cm, 1 σ)
ALGO	4.51	5.39	1.58
NLJB	4.71	4.91	3.69
PENT	4.29	6.23	9.05
PIE1	4.85	4.91	9.38
USR1	4.45	4.45	5.97
USR2	3.74	3.84	8.56
USR3	5.02	5.44	3.66
USR4	4.45	4.41	5.97
USR8	4.90	5.10	7.27
USR9	5.12	5.84	3.45
ALBH	4.46	7.17	9.92
JPLM	5.55	5.20	12.4
MDO1	5.80	5.56	8.97
QUIN	4.11-	5.24	11.2
STJO	7.76	9.48	7.67
USR5	7.69	7.55	5.84
USR6	6.12 -"	5.73	7.91
USR7	6.85	8.00	13.1
WEST	5.40	6.70	3.57
YELL	8.84	12.9	11.5

Table 5: Results of the WAAS user positioning simulation. The numbers show the RMS in the eastern, northern and vertical components of the point positioning history of the simulated WAAS users. The first block shows the users inside the network whereas the second block shows the peripheral users.

$$\frac{\partial r_u^k}{\partial L} = \frac{d}{r_u^k} = \sin \theta, \quad (2)$$

where θ is the angle between the line of sight of user u to satellite k and the direction of line h .

Since the GPS satellites orbit at a very high altitude, the angle θ is small (less than 14 degrees); hence, the nondifferential User Range Error (URE) is more sensitive to changes in radial position of the satellite than to along- and cross-track changes. However, in the differential case the opposite is true. That is to say, the range difference between the users u and monitor station m (see Fig. 6) is more sensitive to along-track satellite motion than to radial motion. Mathematically the sensitivities of the differential range are given (for the 2-D case) by the difference of the partials of r_u^k and r_m^k as given by Eqs. (1) and (2). The maximal sensitivity of the differential range Δr ,

$$\Delta r = |r_m^k - r_u^k|,$$

to a radial error occurs in the configuration depicted in Fig. 6, where the monitor receiver m is directly below

the satellite and the user u is located at the maximal distance possible (≈ 7430 km). This results in the angle $\theta \approx 13.8^\circ$. Therefore, the sensitivities of the differential range for this worst case are given by

$$\frac{\partial \Delta r}{\partial H} = \frac{\partial r_m}{\partial H} - \frac{\partial r_u}{\partial H} \Big|_{(1)} |\cos(0) - \cos(13.8)| = 0.03, \quad (3)$$

$$\frac{\partial \Delta r}{\partial L} = \frac{\partial r_m}{\partial L} - \frac{\partial r_u}{\partial L} \Big|_{(2)} |\sin(0) - \sin(13.8)| = 0.24. \quad (4)$$

It can be seen in this "worst radial sensitivity" case that the sensitivity to the lateral component of the ephemeris error is eight times greater than the radial component; a 1-m error in the radial ephemeris component causes a 3-cm error in the differential range, whereas a 1-m error in the lateral ephemeris component (along-track) causes a 24-cm error in the differential range. On the other hand, the worst case for the lateral sensitivity occurs when the satellite is located in the mid-point distance between the monitor station and the user, and the monitor station and the user

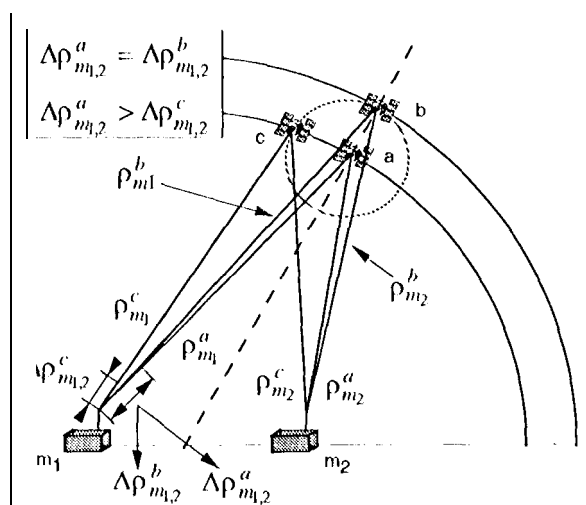


Figure 4: Differential GPS tracking sensitivity. A single satellite is being tracked by a couple of stations m_1, m_2 that combine their individual range measurements to form a differential range measurement $\Delta \rho_{m1,2}$. The differential range is insensitive to radial satellite motion (position change from a to b), and can only sense transversal motion (position change from a to c).

are located at both sides of the Earth's limb as viewed by the satellite. In this case a 1-m ephemeris lateral (along-track) error with a 7420-km baseline between stations results in 34-cm differential range error. The radial and cross-track (in 3-D) sensitivities would be zero in this case.

It is an widespread misconception that in WADGPS only the radial component of the satellite is of interest. On the contrary, with dynamical orbit estimation, the radial orbit error will be up to three times smaller than the horizontal error, hence the radial error will add (Yunck et al. 1995) less than 1% to the ephemeris component of the UDRE and can be ignored. Thus only the lateral (cross-track and along-track) satellite error components are of interest.

3.3 Separation of ephemeris and clock biases

Another important aspect of the orbit estimation problem is the weak separation of satellite position errors and clock errors when no dynamical informa-

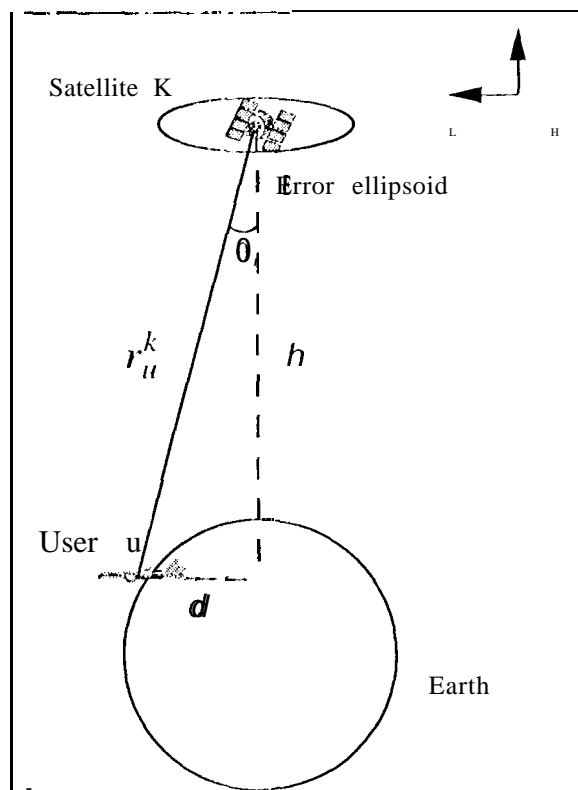


Figure 5: Sensitivities of the UDRE and UDRE due to radial L and lateral H ephemeris errors.

tion is used. A station tracking an orbiting satellite with range measurements over a period of time can use the fact that the satellite moves in a dynamically prescribed orbit to measure the period of the orbiting satellite. This period is related (directly in the case of a circular orbit) to the orbiting altitude of the satellite. This extra information can be used to determine what portions of the range bias are due to ephemeris errors versus clock errors. If the satellite dynamics is ignored, there is no way of distinguishing both biases, and only the sum of the two contributions can be estimated. This concept is illustrated in Fig. 7.

If no dynamics is used, the error ellipsoid of the orbit determination is prolate in the differential mode; that is, there is more error in the radial direction (the direction that cannot be observed) than in the cross- or along-track directions. When dynamical information is incorporated into the problem, the uncertainty of the radial component of the orbit is readily constrained by Newtonian motion. Although the radial component is

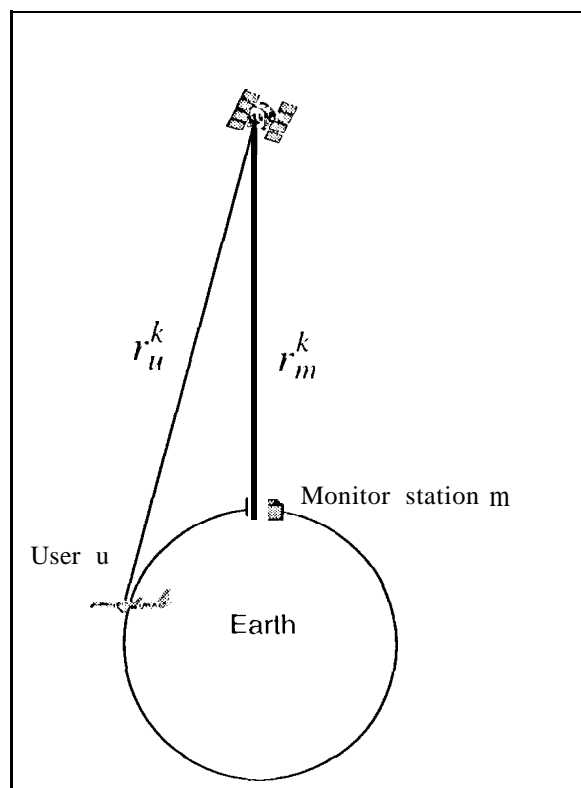


Figure 6: The worst case of URE due to radial error occurs when the monitor station is below the tracking satellite and the user is located at the Earth's limb.

poorly observed, it is related to the two other observed components by dynamical relationships. In this (dynamical) case, the ellipsoid error assumes its proper oblate shape as the results shown in Tables 2 and 3 confirm.

As an exercise, an orbit estimation was performed using the WAAS network of stations presented before. In this estimation no dynamical information was used, i.e., the estimation process was based purely on geometry. Again the resulting orbit was compared with the JPL precise orbit for the same day and the differences plotted. The differences in orbit components (radial, cross-track and along-track) are shown in Table 6. It is clear that the dominant error is in the radial direction, creating the expected prolate ellipsoid error. The radial component of the orbit has also absorbed some of the clock bias errors, for as mentioned before there is no way to distinguish the ephemeris contribution from the clock contribution to the range error unless dynamical information is introduced in the problem.

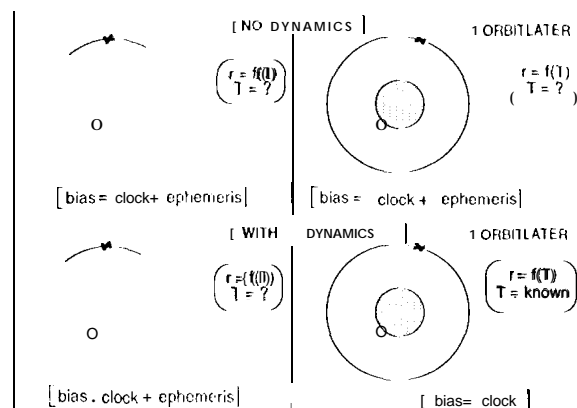


Figure 7: Dynamical vs. nondynamical orbit estimation.

The WAAS Nondynamical Orbit Accuracy	
Orbit component	Accuracy (m, 1σ)
Radial	193
Cross-track	38.8
Along-track	43.7

Table 6: The WAAS nondynamical orbit accuracy. The accuracy is established as the difference between the orbit estimated using the WAAS stations not using dynamical information and the JPL precise ephemerides over the service area of the WAAS network.

This fact, together with an estimated GDOP (as the stations are viewed by the satellite) of near 200 with pseudorange noise of approximately 40 cm, accounts for the large orbital error. It can also be appreciated that when no dynamical information is used, the orbit estimation cannot propagate accurately the orbit outside the WAAS network area.

Another important aspect is that when no dynamical information is used, it is better to follow the strategy that the Stanford University uses, in which ephemeris errors and clock biases are solved simultaneously. Although the independent estimates of these parameters are not accurate, the overall pseudorange correction is very satisfactory as the Stanford flight trials show (Walter et al. 1994). In fact, a simulation shows that when no dynamical information is used, and a slow/fast correction scheme is exercised, the vertical error (just due to orbit error) is on the order of 571 cm.

(1 σ) with a noticeable degradation on the periphery of the network⁸. This result is contrasted in Table 7 with the much better results obtained in the Stanford University simulation and flight trials (Walter et al. 1994).

The algorithm implemented by Stanford University in its flight trials makes use of minimum-norm solution without *a priori* constraints in the solution of the ephemeris and clock errors (Ceva 1995, Tsai et al. 1995). On the other hand, the Stanford Simulation presented in Pullen, Enge & Parkinson (1995), that considers a network that expands over the continental U. S., makes use of *a priori* constraints and also uses a Kalman filter implementation. The fact that when a WAAS network is expanded from a local region (California and Nevada in the case of the Stanford network) to the entirety of the continental U. S. demands the use of *a priori* constraints is in agreement with the result obtained at JPL. Suffice to say that when *a priori* constraints of a couple of meters are added to the non-dynamical orbit estimation, the 3-D RSS of the orbit error (as compared with the JPL precise ephemerides) is in the order of 9 meters (that contrasts with the 3-D RSS of 200 meters obtained when no *a priori* information is used).

3.4 Conclusion

Differential techniques lose sensitivity to radial orbit errors and must use dynamical information to recover properly the missing information from the observed transverse components. The ephemeris contribution to UDRE is dominated by the lateral (along-track) ephemeris errors and not radial ephemeris error. As mentioned in SCc. 2.3, the ability to separate correctly clocks and ephemeris errors permits the use of the slow/fast, scheme that is required in the FAA WAAS specifications. The ability to separate these two error sources adds integrity to the system by enabling the detection of errors in either the estimates of ephemeris biases or clock biases.

4 The Real-Time Aspect

The WAAS must operate in real-time. In the case of the slow corrections, they must be broadcast every five minutes. That means that the corrections must

⁸Note that the fast correction will always absorb part of the ephemeris error that is left after the slow correction is applied.

be computed, verified, packaged and broadcast in less than five minutes.

Table 8 shows the computational times of the complete algorithm presented on an HP 9000/755 workstation with a 26-Megaflops (Megaflop per second) performance. The computational times presented do not include estimates of the time that the system will require for data validation, verification, and input/output protocols.

The assumption in the calculations presented are:

1. Orbit integration.
 - (a) Integration of 24 GPS satellites with the full model described in Section 2.1.
2. Slow correction generation.
 - (a) 9 state parameters for each of the 27 satellites (24 GPS satellites and 3 GEO satellites) i.e., position, velocity, clock, Y bias and solar scale factor.
 - (b) 2 state parameters for each of the 24 WRSs i.e., clock and tropospheric bias.
3. The fast (pseudorange) correction.
 - (a) 24 GPS satellites.
 - (b) 24 WRSs with 12-channel receivers.

Computational Times	
Task	Execution Time
Integrate 24 orbits for 5 min; Compute predicted pseudoranges	< 0.5 sec
Slow (5 min) orbit corrections (pseudorange only)	< 1.9 sec
Slow (5 min) orbit corrections (pseudorange and phase)	< 20 Sec
1 sec fast pseudorange correction	< 50 msec

Table 8: Computational times on HP 9000/755 workstation.

It can be seen that the ephemeris prediction and slow correction calculation take (not including data validation, verification, and input/output protocols) less than 2.5 seconds. Thus the dynamical orbit estimation algorithm would easily meet the WAAS time specifications.

User Positioning Accuracy with a Nondynamical Orbit Estimation		
Stanford University	Stanford	Univ. Slow/Fast Correction
Simulation (cm, 2σ)	Flight Trials (cm, 2σ)	Simulation (cm, 1σ)
341	300	571

Table 7: User positioning accuracy with a nondynamical orbit estimation. The Stanford University simulation and flight trials, in which ephemeris and clock errors are solved simultaneously, are contrasted with the results of a simulation in which the ephemeris and clock errors are solved using a slow/fast correction scheme. The Stanford University approach proves much superior when a nondynamical orbit estimation is implemented.

The packing and transmission times of the correction message can be based on the Stanford experience (Walter et al. 1994), where the whole RTCA SC 159 WAAS message is sent in 27 milliseconds.

Finally it is important to note that although the state-of-the-art models used in the dynamical orbit estimation are very sophisticated, they are well understood and the computational time that they demand easily meets the WAAS specification.

5 Summary of Conclusions

5.1 Summary of conclusions

- A nine-state vector, i.e., position, velocity, clock bias, Y bias and solar pressure scaling factor can accurately characterize the GPS satellites.
- A continental U. S. WAAS network can estimate GPS orbits that are a factor of four better than the broadcast orbits.
- The orbit accuracy improvements lead to a user positioning improvement of a factor of four over the broadcast orbits (excluding nonephemeridal errors).
- With the use of dynamics in the orbit estimation process, the ephemeris and clock biases can be properly separated, thus accommodating the FAA WAAS scheme of slow and fast corrections.
- The orbital dynamical models implemented permit the propagation of the last orbital estimate, to allow future predictions without new measurements, hours ahead (well over 10 minutes) with little or no loss of accuracy. This indicates that perhaps less sophisticated techniques, whose pre-

diction would be good only in the 10-minute range, could be used in a WAAS scenario.

- The ability to separate ephemeris biases from clock biases adds integrity to the system by introducing the capability to detect errors in the estimate of either parameter.
- The dynamical orbit estimation process, the slow correction generation, and its broadcast can be done in 2.5 seconds on an HP 9000/755 workstation with a 26-Megaflops performance. This estimate does not include the time that the system will require for data validation, verification, and input/output protocols. However, since at least 5 minutes are available real-time performance of the dynamical orbit estimation is easily achievable in a WAAS scenario.

Acknowledgements

The work described in this paper was carried out in part by the Jet Propulsion Laboratory, California Institute of Technology, under contract with the National Aeronautics and Space Administration (NASA) and by the Stanford University under NASA grant # NAS8-36125 and under Federal Aviation Administration (FAA) grant # 93-G-004/FAA.

References

- Bierman, G. (1977), *Factorization Methods for Discrete Sequential Estimation*, Academic Press.
- Ceva, J. (1995), Real-time dynamical GPS ephemeris prediction for WAAS applications, Engineer's thesis, Stanford University, Department of Aeronautics and Astronautics, Stanford, CA 94305.

- FAA (1994), Wide Area Augmentation Systems (WAAS) specifications, Technical report, Department of Transportation.
- Fliegel, H. & Gallini, T. (1992), 'Global Positioning System radiation force model for geodetic applications', *Journal of Geophysical Research* **97**(B1), 559-568.
- Grafarend, E. & Schaffrin, B. (1986), General classes of equivalent linear models by nuisance parameter elimination: applications to GPS observations, in 'Proceedings of the Fourth International Geodetic Symposium on Satellite Positioning', Vol. 1, Austin, Texas, pp. 721-733.
- Kee, C. (1993), Wide Area Differential GPS (WADGPS), PhD thesis, Stanford University, Department of Aeronautics and Astronautics, Stanford, CA 94305.
- Kiang, D., Schutz, B. & Watkins, M. (1995), 'On the structure of geometric positioning in GPS measurements', *Manuscripta Geodaeica*. In revision.
- Mannucci, A., Wilson, B. & Edwards, C. (1993), A new method for monitoring the Earth's ionospheric total electron content using the GPS Global Network, in 'Proceedings of the ION GPS 93', The Institute of Navigation, Salt Lake City, Utah.
- Mannucci, A., Wilson, B. & Yuan, D. (1994), An improved ionospheric correction method for Wide-Area Augmentation Systems, in 'Proceedings of the ION GPS 94', The Institute of Navigation, Palm Springs, California.
- Nerem, R. (1994), 'Gravity model development for TOPEX/POSEIDON: Joint gravity models 1 and 2', *Journal of Geophysical Research* **99**(C12), 24383-24404.
- Newhall, X., Standish, E. & Williams, J. (1983), 'DM-102: a numerically integrated ephemeris of the moon and planets spanning forty-four centuries', *Journal of Astronomy and Astrophysics* pp. 150-167.
- Pullen, S., Ping, P. & Parkinson, B. (1995), A new method for coverage prediction for the Wide Area Augmentation System (WAAS), in 'Proceedings of the 51st ION Annual Meeting', Colorado Springs, Colorado, pp. 501-513.
- Tsai, Y. et al. (1995), Evaluation of orbit and clock models for real-time WAAS, in 'Proceedings of the National technical meeting', The Institute of Navigation, Anaheim, California, pp. 539-547.
- Wahr, J. (1981), 'Body tides on an elliptical, rotating, elastic and oceanless Earth', *Journal of Royal Astronomical Society* **64**, 677-703.
- Walter, T. et al. (1994), Flight trials of the Wide-Area Augmentation System, in 'Proceedings of the 1994 ION GPS Meeting', Salt Lake City, Utah, pp. 1537-1546.
- Watkins, M. et al. (1994) 'The JGM-3 gravity model, In preparation.
- Wells, D., Doucet, K. & Lindholm, W. (1986), 'First order geodetic GPS network design: some considerations, in 'Proceedings of the Fourth International Geodetic Symposium on Satellite Positioning', Vol. 1, Austin, Texas, pp. 801-819.
- Wu, S. et al. (1990), Global positioning system (GPS) precision orbit determination (POD) software design, Technical report, Jet Propulsion Laboratory, JPL, internal report JPL D-7275.
- Yunch, T. et al. (1995), A robust and efficient new approach to real time Wide Area Differential GPS navigation for civil aviation, Technical report, Jet Propulsion Laboratory, JPL, internal report JPL D-12584.
- Zumkehrge, J. & Bertiger, W. (1996), *GPS: Theory and Applications*, Vol. 1 of *AIMA Educational Series*, American Institute of Aeronautics and Astronautics, chapter 2.
- Zumkehrge, J. et al. (1995), IGS analysis center 1994 annual report, Technical report, International GPS Service for Geodynamics. In press.